AMERICAN SOCIETY OF CIVIL ENGINEERS FOUNDED 1852

PREPRINT 81-525

$2.00

SOME LIMITATIONS OF DAM-BREACH FLOOD ROUTING MODELS

D. L. Fread

ASCE St. Louis, Missouri October 26–31, 1981

This preprint has been provided for the purpose of convenient distribution of information at the convention. To defray, in part, the cost of printing, a convention price of $2.00 to all registrants has been established. The post-convention price, when ordered from ASCE headquarters will be $2.00 while the supply lasts. For bulk orders (of not less than 200 copies of one preprint) please write for prices.

No acceptance or endorsement by the American Society of Civil Engineers is implied; the Society is not responsible for any statement made or opinion expressed in its publications.

Reprints may be made on condition that the full title, name of author, and date of preprinting by the Society are given.

SOME LIMITATIONS OF DAM-BREACH FLOOD ROUTING MODELS

By Danny L. Fread[1], M. ASCE

INTRODUCTION

A flood which is caused by the failure (breach) of a dam is much larger than any of the previous floods that originated from the runoff of rainfall and/or snowmelt; and, its consequences are often catastrophic if human development exists downstream of the dam. Our ability to predict the magnitude and timing of the dam-breach flood is of paramount importance for purposes of: 1) planning and decision making concerning dam safety, 2) contingency evacuation planning, and 3) real-time flood forecasting.

During the last decade some major improvements were made in the mathematical techniques (models) used to predict the continually changing magnitude and velocity of the dam-breach flood wave. Advancing beyond the simple, classical mathematical treatment of dam-breach waves of St. Venant (7), Ritter (22), and Schoklitsch (24), models were developed which by using simple storage routing concepts considered the effects of the downstream valley friction and storage volume on the wave's propagation, e.g., HEC (11), Snyder (25), Keefer and McQuivey (14), Keefer and Simons (15), and Brevard and Theurer (2).

Other models requiring large, high-speed computers were developed which utilized the more complex and accurate one-dimensional equations of unsteady flow for routing the dam-breach flood wave through the downstream valley. Included among these were Cunge (6), Balloffet, et al. (1), Price and Garrison (19), Price, et al. (20), Thomas (26), Fread (8,9), Rajar (21), and Chen and Armbruster (3). Also, models of this type but considerably simplified for use with desk calculators were developed by Sakkas and Strelkoff (23) and Wetmore and Fread (28). Some models (9,15) also considered the effects of other dams and/or bridge-embankments in the downstream valley.

---

[1]Senior Research Hydrologist, Hydrologic Research Laboratory, National Weather Service, NOAA, 8060 13th St., Silver Spring, MD.

Most of the models relied on the classical methods of St. Venant and Schoklitsch to determine the magnitude of the wave at its point of origin, the breached dam. Simple storage concepts were used to determine its assumed triangular shape, and the formation of the breach was assumed to take place instantaneously. The models of HEC (11), Price and Garrison (19), Fread (8,9), and Wetmore and Fread (28) attempted to treat the breach formation for an earthen dam more realistically by approximating its dynamic development. Also, the integrated effects of reservoir inflow and storage characteristics and the downstream valley backwater on the magnitude and shape of the dam-breach wave were considered by Fread (8,9) and HEC (11).

Notwithstanding the improvements in the dam-breach flood models that have evolved over the last decade, several sources of error still limit the accuracy of the most advanced models to predict the magnitude and time of occurence of the flooding at any specified location downstream of the dam. The errors are due to our inability at the present time to accurately answer the following questions: When will a dam fail? When and to what extent will a dam be overtopped? What is the size, shape, and time of formation of the breach? What is the storage volume and hydraulic resistance of the downstream channel-valley? Will debris (uprooted trees, etc.) and sediment (entrapped behind the dam and in the stream channel) transported by the flood wave significantly affect its propagation? Can the wave be approximated adequately by the one-dimensional flow equations?

MODEL LIMITATIONS

Comparisons have been made of several dam-breach flood routing models (3,8,9,14,16,21,26,28) with observations from some actual dam-breach floods, e.g., the Teton, Toccoa, Laurel Run, Buffalo Creek floods. The comparisons indicate that even the most advanced models have limitations in the accuracy of the predicted flood crest profiles. Errors are usually one to two feet or more for all of the models, even when the actual breach geometry is specified as input to the models. The factors which can cause errors in the prediction accuracy of the most advanced dam-breach flood models are several.

Dam Failure. - Many times the most difficult prediction is whether or not the dam will fail. Certainly in cases where dam failure is caused by piping, seepage, slides, or seismic disturbances prediction of if and when a dam will fail is not within the capability of the models. Such causes of failure constitute somewhere between 40 and 50 percent of the total number recorded failures (12,17). Failures caused by overtopping of the dam due to inadequate spillway capacity total about 30 to 35 percent of the dam failures with the remaining 15 to 30 percent classified as miscellaneous causes.

Although overtopping can be predicted it is subject to error due to the limitations of the hydrologic model chosen to predict the inflow to the reservoir from rainfall and/or snowmelt. Errors in observed or predicted areal precipitation (the primary input to hydrologic models) is considerable. Also, the use of statistically generated probable maximum precipitation or probable maximum runoff is beset with considerable uncertainties.

Notwithstanding the errors in the inflow to the reservoir, the determination of the extent of overtopping (depth of flow over the crest and the duration of the overtopping flow) which is required for breaching to occur is not an inherent feature of the dam-breach flood models. Some attempts were made to develop erosion models for earthen dams (5,10) however, these were not very adequate. A recent effort by Ponce and Tsivoglou (18) may hold some promise although the difficulties of nonhomogeneity and lack of detailed data for most earthen dams may limit the applicability of this approach. Almost all of the dam-breach models do not address the question of when failure from overtopping commences although a few (8,9,11) utilize a specified depth of overtopping flow to start the formation of the breach.

Breach Characteristics. - A significant source of error is the size, shape, and time of formation of the breach. The few models (8,9,11) which attempt to include the dynamic characteristics of the breach require the user to specify the terminal width, shape and a time of formation which is assumed linear. This information must be obtained from historical dam failures and then applied to the dam being modeled using sound engineering judgement by considering the type of dam (earthfill, rockfill, concrete gravity or arch), the dam's material properties, the cause of failure, the height of the dam, the reservoir volume, and any other special characteristics which might affect the breach formation. An erosion model (18) may in certain instances increase the accuracy of the breach prediction.

Of the three breach characteristics, the shape is least important. Time of formation becomes increasingly insignificant as the reservoir volume becomes very large. The peak discharge (Q_p) emanating from a time-dependent breach can be approximated (28) as:

$$Q_p \simeq 3.1\ W\ [C/(\tau+C/\sqrt{H})]^3 \qquad (1)$$

$$\text{where:} \quad C = 23.4\ S_a/W \qquad (2)$$

in which W is the average breach width (ft), τ is the time (hrs) of breach formation (the time in which the flow passage is enlarging), H is the height (ft) of the dam, and S_a is the reservoir surface area (acres) at the dam crest. Using Eq (1) the peak discharge can be determined for various values of τ, and the sensitivity of Q_p to errors in the time of failure can be determined readily. For example

if, τ=1.5 hr, W=150 ft, S_a=1936 acres, H=262 ft which approximates the Teton dam failure, values of Q_p as a function, of τ are given in Table 1.

Table 1. - Peak Discharge (Q_p) Variations with Time of Failure (τ)

Q_p(cfs)	τ (hr)	Error(%)
1,977,589	0.0	+ 26.1
1,756,766	0.75	+ 12.1
1,567,817	1.5	0.0
1,263,868	3.0	- 19.3

If S_a were 193,600 acres, the error for τ=0. would only be +.2%; whereas, if S_a were only 193.6 acres, a τ=0. would produce a much larger error in Q_p of +487.5%.

Eq (1) can also be used in a similar manner to acertain the effect of error in the average breach width (W). This is a most important source of error. It is most difficult to determine for concrete gravity dams, while its probable value for concrete arch dams is near the full width of the dam. For earthfill dams there is evidence (9,12) that W is somewhat correlated to the dam height (H), i.e.,

$$0.5\ H \leq W \leq 3\ H \qquad (3)$$

At this time the best analysis that can be achieved with such uncertainties in the breach properties is to make two predictions, first using a maximum probable W and minimum probable τ and then using a minimum probable W and maximum probable τ. The first produces a maximum expected downstream flooding while the second produces a minimum expected flooding. This is illustrated in Fig. 1 in which the peak discharge profile is shown for four different conditions. The two lower profiles are associated with the approximated actual downstream valley (Teton-Snake River) dimensions while the two upper profiles are for a narrow canyon (approx. 1100 ft wide) extending throughout the 60 mile downstream reach.

Four properties of dam-breach floods are illustrated by the profiles shown in Fig 1. First, in each case significant differences in the predicted peak flow in the vicinity of the dam are significantly reduced as the flood propagates downstream. Second, the differences are more rapidly reduced for the actual valley (which is very wide and flat having a maximum inundated width of about nine miles) than for the narrow canyon. Third, the peak discharge is rapidly attenuated as the flood advances downstream, and fourth, the peak flow is attenuated more in the wide valley than in the narrow canyon. These general properties are applicable to dam-failure floods; however, the degree of trend of the first three becomes less

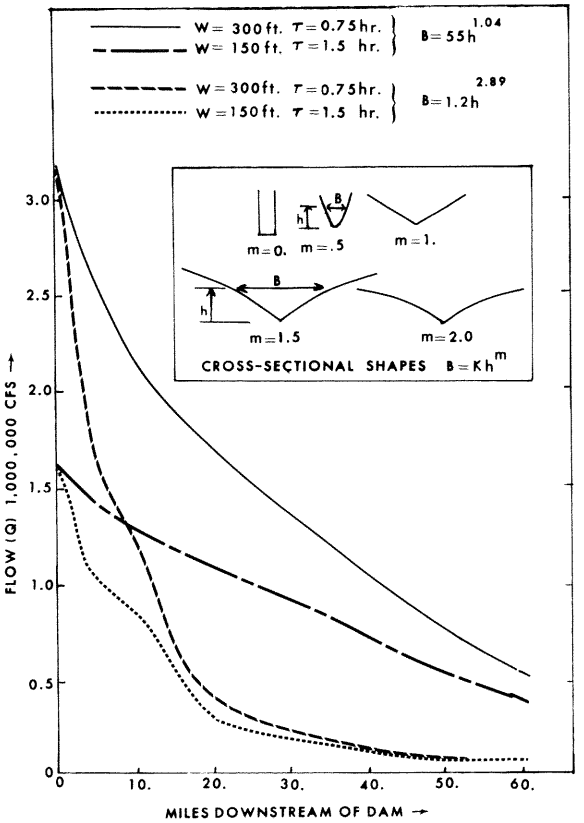

FIG.1- VARIATION OF PEAK FLOW DOWNSTREAM OF DAM

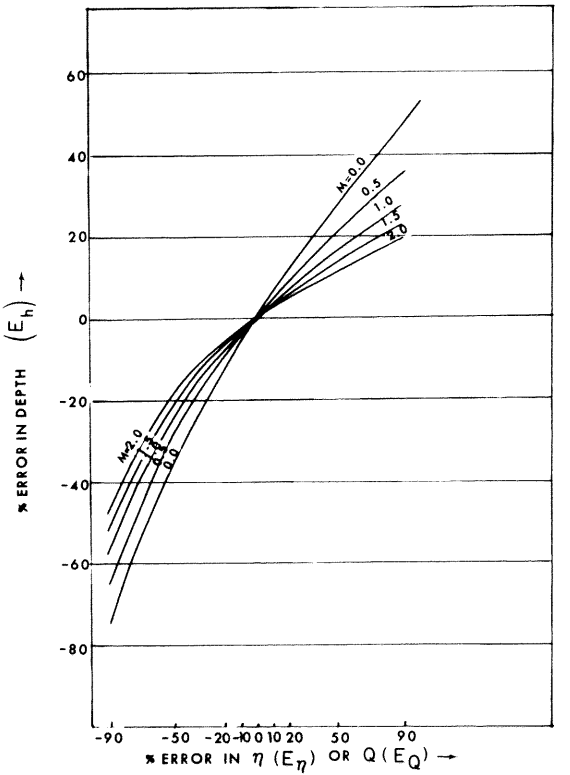

FIG.2-ERROR IN FLOOD DEPTH CAUSED BY ERROR IN ROUGHNESS (η) OR FLOW (Q) FOR VARIOUS SHAPED SECTIONS HAVING STEADY FLOW

as the reservoir volume increases. This is due to the fact that attenuation of the peak discharge becomes less as the volume of the flood wave increases in relation to a fixed storage volume of the downstream valley.

The first principle, the dampening of initial differences in the peak discharge as the flood propagates downstream, enables prediction accuracy to increase in the downstream direction.

The errors in the routed discharge may be transformed into errors in flow depth (h), which are more meaningful, by either using actual depth-discharge rating curves or in the following way. Let the average cross section of the downstream channel-valley be described as:

$$B = kh^m \tag{4}$$

$$A = \frac{kh^{m+1}}{m+1} \tag{5}$$

in which B is the width, A is the cross-sectional area, and k and m are fitting coefficients (see Fig. 1). Then from the Manning Equation,

$$h = (Q/a)^b \tag{6}$$

where: $$a = 1.49\ S^{1/2}\ k/[n(m+1)^{5/3}] \tag{7}$$

$$b = 3/(3m + 5) \tag{8}$$

in which S is the channel-valley slope and n is the Manning roughness coefficient. Using Eq (6), the following ratio may be developed:

$$h_e/h = (Q_e/Q)^b \tag{9}$$

in which the subscript (e) designates quantities possessing some error. Since the fitting coefficient m is present in Eq (9), the general shape of the cross section as determined by m as shown in Fig 1. must be considered. An expression for the percent error in depth (E_h) may be developed in terms of the ratio h_e/h, i.e.,

$$E_h = 100\ (h_e/h - 1) \tag{10}$$

and a similar expression for the percent error in discharge (E_Q), i.e.,

$$E_Q = 100\ (Q_e/Q - 1) \tag{11}$$

Furthermore, the error term (E_h) may be plotted as shown in Fig. 2 against the percent error in the discharge (E_Q) for a range of cross-sectional shapes. Fig. 2 shows that the relationship between E_h and

E_Q is nonlinear. For example, if E_Q = +50% and m=2.0, E_h is determined from Fig. 2 to be about 9.5%. The tendency for an error in flow to yield a smaller error in depth is characteristic of all curves in Fig. 2; this is helpful in promoting prediction accuracy of dam-breach flood routing models. Fig. 2 is based on steady flow, therefore it is strictly applicable only for discharge errors existing after flood routing computations have been performed.

Cross-Sectional Area. - Errors to some extent are always present in the description of the cross-sectional properties (width and area as a function of flow depth) of the downstream channel-valley. These are: errors in sampling, errors in field measurements, and errors inherent in the assumed linear variation between contour intervals of topographic maps. The first two errors are associated with the use of field measured cross-sections while all three errors can occur when using topographic maps for determing cross-sections for a dam-breach flood routing model.

The cross-sectional volume error due to the sampling interval can be eleminated if planmetered surface areas between two selected cross-sections are used to compute the properties of an average section placed between the selected sections. The width ($\overline{B}$) of the average section can be determined from a distance-weighting relationship, e.g.,

$$\overline{B} = (2\ S_c - B_1\Delta x_1 - B_2\Delta x_2)/(\Delta x_1 + \Delta x_2) \tag{12}$$

in which S_c is the surface area contained between contour lines of the same elevation and located on opposite sides of the valley and bounded on the ends by the selected sections designated by subscripts 1 and 2. Also, Δx_1 and Δx_2 are the respective distances (ft) from the first end section to the location of the average section, and from the average section to the second end section. Field measured properties of the cross section within the banks of the channel are needed to reduce errors in this portion of the cross-section since topographic maps do not extend below the typical water level. However, in many cases peak dam-breach flows would have small errors since the in-bank area is a small percentage of the flooded over-bank area.

The error associated with the assumed linear variation between contour intervals (Δh) is illustrated in Fig. 3. An approximate expression for the ratio of A_e/A is given by the following:

$$A_e/A \simeq 1.0 + \overline{P}\ (m+1)\ (\Delta h/h_p)^m \tag{13}$$

where: $$\overline{P} = \sum_{i=1}^{N} e_i = \sum_{i=1}^{N} \Delta A_i/A_i' \tag{14}$$

$$N = 2h_p/\Delta h \tag{15}$$

$$h_p = (Q_p/a)^b \tag{16}$$

in which Δh is the contour interval, h_p is the maximum depth in the section, ΔA_i and A_i' are defined in Fig. 3, Q_p is the maximum discharge at the section while m,a, and b are defined as in Eqs (4-5). A realistic maximum value for the ratio (A_e/A) can be obtained from Eq (13) by using $\overline{P} = 0.4$. From Eq (13) it is seen that larger values of A_e/A and therefore larger errors in the cross-sectional area are directly proportional to m and to the term $(\Delta h/h_p)^m$. The latter term represents the ratio of contour interval to peak depth. Therefore as the contour interval increases, the error increases. Also, the error increases as the ratio $(\Delta h/h_p)$ increases and since h_p is related to the dam height (H) through Eqs (1) and (16), the error increases as the ratio $\Delta h/H$ increases. The error is related to the cross-sectional shape by the exponent m in the term $(\Delta h/h_p)^m$.

Using Eq (6), the following ratio may be developed:

$$h_e/h = (A_e/A)^{5b/3} \tag{17}$$

and an expression for percent error in the cross-sectional area (E_A) is given by:

$$E_A = 100\ (A_e/A - 1) \tag{18}$$

The error term E_A may be plotted as shown in Fig 4. against the percent error (E_A) for a range of channel shapes. The relationship is linear for m=0 and becomes more nonlinear as m increases. As m increases the errors become more damped, i.e., if E_A = +50% and m = 2.0, E_h is only +20%.

Flow Resistance Coefficients. - Errors in the flow resistance coefficients are due to such factors as: (1) dam-breach flows which are relatively large occur in previously unflooded areas; thus previous flows are not very useful in computing the flow resistance coefficients; (2) the inundated area often contains more flow resistance in the form of trees, houses, etc. which are not typical of the resistance encountered by most normal floods; (3) the flood-plain flow short-circuits across a meandering channel (4) causing some additional flow resistance; (4) debris (trees, etc.) uplifted and transported by the flood may become impinged on permanent obstructions causing additional undefined flow resistance; and (5) sediment entrapped behind the dam and released during the failure may slightly reduce the flow resistance when it is deposited on the flood plain (4).

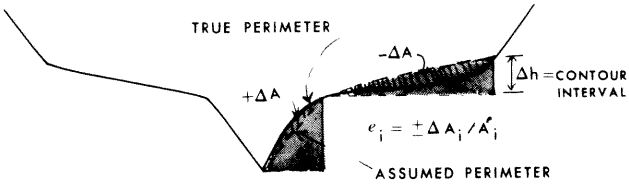

FIG. 3 - CROSS SECTION SHOWING ERROR $\left(e_i = \pm \Delta A / A'_i\right)$ DUE TO ASSUMED STRAIGHT-LINE VARIATION BETWEEN CONTOUR INTERVALS

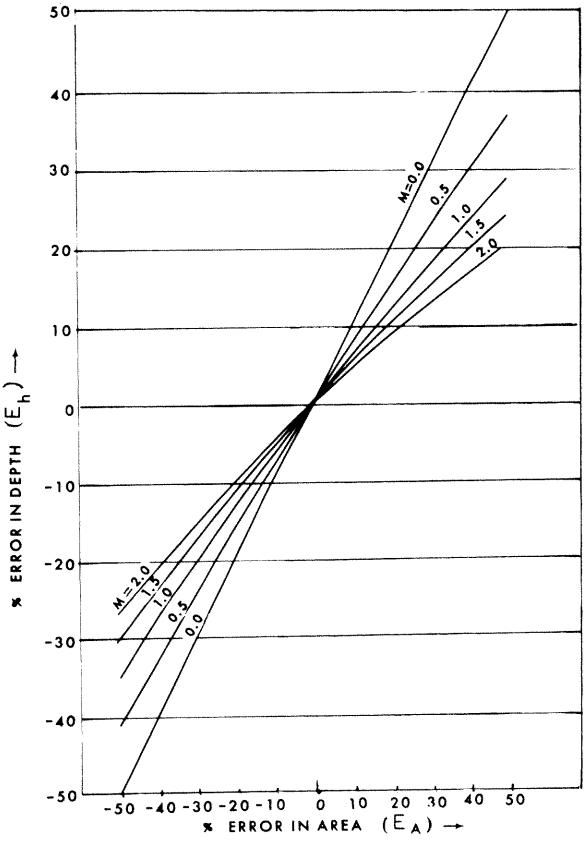

FIG. 4 - ERROR IN FLOOD DEPTH CAUSED BY ERROR IN CROSS-SECTIONAL AREA FOR VARIOUS SHAPED SECTIONS HAVING STEADY FLOW

The errors associated with the first two factors may be reduced by using a type of Colebrook-White frictional expression which separately approximates effects of submerged and partially submerged objects on the flow resistance (27). The computed Darcy friction factor (f) can then be changed to the more popular Manning n coefficient by using the relation,

$$n = f^{1/2} h^{1/6} / 10.8 \tag{19}$$

The effect that the total error in the frictional resistance (expressed in terms of the Manning n) has on the flood depth can be obtained by using Eq (6). Thus,

$$h_e/h = (n_e/n)^b \tag{20}$$

An expression for the percent error in the Manning n (E_n) may be developed, i.e.,

$$E_n = 100\ (n_e/n - 1) \tag{21}$$

If E_n is plotted against E_h as shown in Fig. 2 it is apparent that the relationship is nonlinear and that errors in the Manning n (E_n) are dampened when transformed into errors in flow depth (E_h) as was also the case with the errors in flow (E_Q). The extent of dampening is directly proportional to the channel shape or the m coefficient of Eq (9). The error dampening characteristic is beneficial for the prediction accuracy of computed depths.

Errors in the Manning n will also have a significant effect on the kinematic celerity (approximate propagation speed) of the flood wave. Using Eq (20), the following celerity ratio can be developed:

$$c_e/c = (n_e/n)^{2b/3 - 1} \tag{22}$$

Eq (22) indicates that errors in the Manning n will produce damped errors in the wave celerity. For example, if E_n = +50% and m = 1.0 the error in the wave celerity would be only -25%. Also, the influence of the cross-section shape factor(m) is very weak in Eq (22).

Debris. - Uprooted trees, demolished houses, cars, fences, and other debris transported by the high velocity flow associated with the dam-breach flood cause unpredictable errors. The debris can increase the frictional resistance coefficients. It may also accumulate at constricted cross sections such as bridge openings where it partially or completely restricts the flow as a temporary dam. This occured during the infamous Johnstown dam-breach flood of 1889. At best, the maximum magnitude of this effect can only be approximated by a dam-breach model (9) which treats the blocked constriction as another downstream dam having an estimated head-

discharge rating which somewhat approximates the gradual flow stoppage and the later possible rapid increase if the debris dam is breached. The errors in dam-breach flow predictions caused by debris dams are not predictable since the occurrance, itself, cannot be predicted.

Volume Losses. - Often in dam-breach floods, where the extremely high flows inundate considerable portions of channel overbank or valley flood plain, a measurable loss of flow volume occurs. This is due to infiltration into the relatively dry overbank material, detention storage losses, and sometimes short-circuiting of flows from the main valley into other drainage basins via canals or overtopping natural ridges separating the drainage basins. Such losses of flow are most difficult to predict; usually they are neglected in the dam-breach models, although the losses can be significant. In the case of the Teton flood where the measured losses amounted to about 25% of the reservoir volume, consideration of the losses (8) decreased the routed peak discharge and depth by 50% and 31%, respectively, at a cross-section which had a shape factor(m) of 0.5 and located 60 miles downstream. The average decrease in peak discharge and depth along the 60 mile reach were about 18% and 7%, respectively.

Sediment Transport. - Sediment entrapped behind a breached dam may be transported along with the breach flow and deposited in the downstream valley. In some cases (4) this can reduce the flow resistance coefficient. Also, degradation of the channel bottom may occur due to the high velocity flow emanating from a breached dam. Degradation increases the cross-sectional area of the channel; however, since the channel area is usually small compared to the flooded overbank area the effect on the total flow would be small.

Complex Flow. - The highly turbulent flow in the reach just downstream of the breached dam may not be adequately described by the equations of one-dimensional flow. Also, dam-breach flow that spreads onto a very wide, flat flood plain is subject to some computational error when treated with one-dimensional routing models. In this case, two-dimensional models (13,29) may provide more accuracy; however, at the present time such models are not sufficiently developed for practical and general application, and are functional primarily as research tools.

CONCLUSIONS

In recent years, significant developments have been made in one-dimensional models to predict the flooding due to breached dams; nevertheless, even the more advanced models are limited in their prediction accuracy. The models, when used to reproduce historical dam-failure floods (3,9,16) in which the breach characteristics (shape, size, time of formation) and/or the breach outflow could be adequately approximated, produced errors of about two feet or more in the profile of the flood crest. When the models are used to predict future dam-breach floods, additional significant errors are introduced through the prediction of the breach characteristics and/or the

breach outflow. Perhaps the greatest error in many applications is determining if indeed a dam will be breached. Other errors in the predicted downstream flooding are due to errors in the downstream cross-sectional volume, estimated flow resistance coefficients, undefined effects of transported debris and sediment, undefined flow volume losses, and complex flows that are not well-suited for one-dimensional flow computations.

The errors associated with the breach characteristics do dampen as the flood propagates downstream, and the degree of dampening depends on the cross-sectional shape and the reservoir volume. Also, the percent error in the computed flow depth is less than the percent error in routed discharge, cross-sectional area, and/or flow resistance. Also, there is a dampening of the error in the wave celerity caused by error in the resistance coefficient. These error properties aid in producing the accuracy that is now achievable with dam-breach flood routing models.

APPENDIX 1. - REFERENCES

1. Balloffet, A., Cole, E. and Balloffet, A.F., "Dam Collapse Wave in a River", Journal of the Hydraulics Division, ASCE, Vol. 100, HY5, pp. 645-665, May 1974.
2. Brevard, J.A., and Theurer, F.D., "Simplified Dam-Break Routing Procedure", Technical Release Number 66, U.S. Dept. of Agriculture, Soil Conservation Service, Engr. Div., 35 pp., 1979.
3. Chen, C. and Armbruster, J.T., "Dam-Break Wave Model: Formulation and Verification", Journal of the Hydraulics Division, ASCE, Vol. 106, HY5, pp. 747-767, May 1980.
4. Chen, Y.H. and Simons, D.B., "An Experimental Study of Hydraulic and Geomorphic Changes in an Alluvial Channel Induced by Failure of a Dam", Water Resources Research, Vol. 15, No. 5, pp. 1183-1188, October 1979.
5. Cristofano, E.A., "Method of Computing Rate for Failure of Earthfill Dams". Bureau of Reclamation, Denver, Colo., April, 1965.
6. Cunge, J.A., "Calcul de Propagation des Ondes de Rupture de Barrage (Computation of Dam-Break Waves)", La Houille Blanche, No. 1, 1970.
7. De Saint-Venant, Barre, "Theory of Unsteady Water Flow, with Application to River Floods and to Propagation of Tides in River Channels", Acad. Science (Paris) Comptes rendus, Vol. 73, pp. 237-240, 1871.
8. Fread, D.L., "The Development and Testing of a Dam-Break Flood Forecasting Model", Proceedings, Dam-Break Flood Modeling Workshop, U.S. Water Resources Council, Washington, D.C., pp. 164-197, 1977.
9. Fread, D.L., "Capabilities of NWS Model to Forecast Flash Floods Caused by Dam Failures", Preprint Volume, Second Conference on Flash Floods, March 18-20, Amer. Meteorological Soc., Boston, Mass., pp. 171-178, 1980.
10. Harris, G.W., and Wagner, D.A., "Outflow from Breached Dams", University of Utah, 1967.

11. Hydrologic Engineering Center (HEC), "Flood Hydrograph Package (HEC-1): Users Manual for Dam Safety Investigation", The Hydrologic Engineering Center, Corps of Engineers, U.S. Army, Davis, Cal., 88 pp., Sept. 1978.
12. Johnson, F.A., and Illes, D.A., "A Classification of Dam Failures", Water Power and Dam Construction, pp. 43-45, Dec., 1976.
13. Katapodes, N., and Strelkoff, T., "Two-Dimensional Shallow Water-Wave Models", Journal of the Engineering Mechanics Division, ASCE, Vol. 105, EM2, pp. 317-334, April 1979.
14. Keefer, T.N., and McQuivey, R.S., "Simplified Routing of Dam Break Waves", Proceedings, IAHR, Vol. 2, San Paulo, Brazil, pp. 325-329, 1975.
15. Keefer, T.N., and Simons, R.K., "Qualitative Comparison of Three Dam-Break Routing Models", Proceedings, Dam-Break Flood Modeling Workshop, U.S. Water Resources Council, Washington, D.C., pp. 292-311, 1977.
16. Land, L.F., "Evaluation of Selected Dam-Break Flood-Wave Models by Using Field Data", U.S. Geological Survey Gulf Coast Hydro Science Center, NSTL Station, Miss., Water-Resources Investigations 80-44, 54 pp., July 1980.
17. Middlebrooks, T.A., "Earth-Dam Practice in the United States", Centennial Transactions, ASCE, Paper No. 2620, pp. 697-722, 1952.
18. Ponce, V.M., and Tsivoglou, A.J., "Modeling Gradual Dam Breaches", Journal of the Hydraulics Division, ASCE, Vol. 107, HY6, Paper No. 16371, June 1981.
19. Price, J.T. and Garrison, J.M., "Floodwaves from Hydrologic and Seismic Dam Failures", Paper presented at ASCE National Water Resources Meeting, January 1973.
20. Price, J.T., Lowe, G.W., and Garrison, J.M. "Unsteady Flow Modeling of Dam-Break Waves", Proceedings, Dam-Break Flood Modeling Workshop, U.S. Water Resources Council, Washington, D.C., pp. 90-130.
21. Rajar, R., "Mathematical Simulation of Dam-Break Flow", Journal of the Hydraulics Division, ASCE, Vol. 104, HY7, pp. 1011-1026, July 1978.
22. Ritter, A., "The Propagation of Water Waves", Ver. Deutsch Ingenieure Zeitschr. (Berlin), Vol. 36, Pt. 2, No. 33, pp. 947-954, 1892.
23. Sakkas, J.G., and Strelkoff, T. "Dam Break Flood in a Prismatic Dry Channel", Journal of the Hydraulics Division, ASCE, Vol. 99, HY12, pp. 2195-2216, Dec., 1973.
24. Schoklitsch, A., "On Waves Created by Dam Breaches", Akad. Wiss. (Vienna) Proc., 126, Pt. 2A, pp. 1489-1514, 1917.
25. Snyder, F.F., "Floods from Breaching of Dams". Proceedings, Dam-Break Flood Modelling Workshop, U.S. Water Resources Council, Washington, D.C., pp. 75-85, 1977.
26. Thomas, W.A., "Calculating and Routing of the Teton Dam-Break Flood", Proceedings, Dam-Break Flood Modeling Workshop, U.S. Water Resources Council, Washington, D.C., pp. 198-227, 1977.
27. Walton, R. and Christensen, B.A., "Friction Factors in Storm Surges Over Inland Areas", Journal of Waterway, Port, Coastal and Ocean Division, ASCE, Vol. 106, WW2, pp. 261-271, May 1980.

28. Wetmore, J.N., and Fread, D.L., "The NWS Simplified Dam-Break Flood Forecasting Model", Proceedings, 5th Canadian Hydrotechnical Conference, Fredericton, Canada, 24 pp., May 1981.
29. Xanthopoulous, T., and Koutitas, C., "Numerical Simulation of a Two-Dimensional Flood Wave Propagation Due to Dam Failure", Journal of Hydraulic Research, IAHR, Vol. 14, No. 4, pp. 321-331, 1976.

APPENDIX 2. - NOTATION

The following symbols are used in this paper:

A = cross-sectional area
A_e = cross-sectional area with error
A_i = cross-sectional area defined in Fig. 3
a = coefficient defined by Eq (7)
B = cross-sectional top width
$\overline{B}$ = cross-sectional top width for average section between two end sections
b = coefficient defined by Eq (8)
C = coefficient defined by Eq (2)
c = kinematic wave celerity
c_e = kinematic wave celerity with error
E_A = percent error in cross-sectional area
E_h = percent error in flow depth
E_n = percent error in Manning n
E_Q = percent error in flow
e_i = error in cross-section
f = Darcy friction factor
H = dam height
h = depth of flow
h_e = depth with error
h_p = depth associated with peak flow at a section
k = fitting coefficient for cross-section (scale factor)
m = fitting coefficient for cross-section (shape factor)
N = integer defined by Eq (15)
n = Manning n
n_e = Manning n with error
$\overline{P}$ = cumulative error ratio for cross-section area
Q = flow
Q_e = flow with error
Q_p = peak flow emanating from breached dam
S = channel-valley slope
S_a = surface area of reservoir at height of dam
S_c = surface area of downstream valley reach between two end sections
W = average width of breach
ΔA_i = cross-sectional area (error)
Δh = contour interval
Δx = distance between end section and average section
τ = time for breach formation

SOME LIMITATIONS OF DAM-BREACH FLOOD ROUTING MODELS

KEY WORDS: Breach, Dams, Failure, Floods, Flood routing, Forecasting, Models, Reservoirs, Rivers

ABSTRACT: During the last decade some major improvements were made in models which predict the changing celerity and magnitude of a flood wave emanating from a breached (failed) dam and propagating through the downstream valley. Such improvements included consideration of the breach dynamics, use of the one-dimensional equations of unsteady flow to route the flood wave through the downstream valley, and consideration of the effects of downstream bridge-embankments, dams, and dead storage areas on the propagating wave. Notwithstanding this, the predictive accuracy of such models can be subject to significant error (two feet or more in the crest profile) due to inaccuracies in the following: 1) the reservoir inflow computed from hydrologic precipitation-runoff models; 2) the breach dynamics which are estimated from previous dam failures; 3) the downstream cross-section properties; 4) the estimated flow resistance coefficients; 5) the neglected effects of transported debris on flow resistance and blockage of constricted cross sections; 6) the neglected infiltration and detention storage losses of flood volume; 7) the neglected sediment transport effects on bottom elevation and flow resistance of the downstream channel-flood plain; and 8) the highly turbulent flows and complex flow patterns not adequately described by one-dimensional flow equations.

REFERENCE: Fread, Danny L., "Some Limitations of Dam-Breach Flood Routing Models," Preprint, ASCE Fall Convention, St. Louis, Missouri, October 26-30, 1981.

SOME LIMITATIONS OF DAM-BREACH FLOOD ROUTING MODELS[a]

By Danny L. Fread[1], M. ASCE

INTRODUCTION

A flood which is caused by the failure (breach) of a dam is much larger than any of the previous floods that originated from the runoff of rainfall and/or snowmelt; and, its consequences are often catastrophic if human development exists downstream of the dam. Our ability to predict the magnitude and timing of the dam-breach flood is of paramount importance for purposes of: 1) planning and decision making concerning dam safety, 2) contingency evacuation planning, and 3) real-time flood forecasting.

During the last decade some major improvements were made in the mathematical techniques (models) used to predict the continually changing magnitude and velocity of the dam-breach flood wave. Advancing beyond the simple, classical mathematical treatment of dam-breach waves of St. Venant (7), Ritter (22), and Schoklitsch (24), models were developed which by using simple storage routing concepts considered the effects of the downstream valley friction and storage volume on the wave's propagation, e.g., HEC (11), Snyder (25), Keefer and McQuivey (14), Keefer and Simons (15), and Brevard and Theurer (2).

Other models requiring large, high-speed computers were developed which utilized the more complex and accurate one-dimensional equations of unsteady flow for routing the dam-breach flood wave through the downstream valley. Included among these were Cunge (6), Balloffet, et al. (1), Price and Garrison (19), Price, et al. (20), Thomas (26), Fread (8,9), Rajar (21), and Chen and Armbruster (3). Also, models of this type but considerably simplified for use with desk calculators were developed by Sakkas and Strelkoff (23) and Wetmore and Fread (28). Some models (9,15) also considered the effects of other dams and/or bridge-embankments in the downstream valley.

---

[a]Presented at the October 26-30, 1981 ASCE Fall Convention, St. Louis, Missouri.

[1]Senior Research Hydrologist, Hydrologic Research Laboratory, National Weather Service, NOAA, 8060 13th St., Silver Spring, MD.

Most of the models relied on the classical methods of St. Venant and Schoklitsch to determine the magnitude of the wave at its point of origin, the breached dam. Simple storage concepts were used to determine its assumed triangular shape, and the formation of the breach was assumed to take place instantaneously. The models of HEC (11), Price and Garrison (19), Fread (8,9), and Wetmore and Fread (28) attempted to treat the breach formation for an earthen dam more realistically by approximating its dynamic development. Also, the integrated effects of reservoir inflow and storage characteristics and the downstream valley backwater on the magnitude and shape of the dam-breach wave were considered by Fread (8,9) and HEC (11).

Notwithstanding the improvements in the dam-breach flood models that have evolved over the last decade, several sources of error still limit the accuracy of the most advanced models to predict the magnitude and time of occurence of the flooding at any specified location downstream of the dam. The errors are due to our inability at the present time to accurately answer the following questions: When will a dam fail? When and to what extent will a dam be overtopped? What is the size, shape, and time of formation of the breach? What is the storage volume and hydraulic resistance of the downstream channel-valley? Will debris (uprooted trees, etc.) and sediment (entrapped behind the dam and in the stream channel) transported by the flood wave significantly affect its propagation? Can the wave be approximated adequately by the one-dimensional flow equations?

MODEL LIMITATIONS

Comparisons have been made of several dam-breach flood routing models (3,8,9,14,16,21,26,28) with observations from some actual dam-breach floods, e.g., the Teton, Toccoa, Laurel Run, Buffalo Creek floods. The comparisons indicate that even the most advanced models have limitations in the accuracy of the predicted flood crest profiles. Errors are usually one to two feet or more for all of the models, even when the actual breach geometry is specified as input to the models. The factors which can cause errors in the prediction accuracy of the most advanced dam-breach flood models are several.

Dam Failure. - Many times the most difficult prediction is whether or not the dam will fail. Certainly in cases where dam failure is caused by piping, seepage, slides, or seismic disturbances prediction of if and when a dam will fail is not within the capability of the models. Such causes of failure constitute somewhere between 40 and 50 percent of the total number recorded failures (12,17). Failures caused by overtopping of the dam due to inadequate spillway capacity total about 30 to 35 percent of the dam failures with the remaining 15 to 30 percent classified as miscellaneous causes.

Although overtopping can be predicted it is subject to error due to the limitations of the hydrologic model chosen to predict the inflow to the reservoir from rainfall and/or snowmelt. Errors in observed or predicted areal precipitation (the primary input to hydrologic models) is considerable. Also, the use of statistically generated probable maximum precipitation or probable maximum runoff is beset with considerable uncertainties.

Notwithstanding the errors in the inflow to the reservoir, the determination of the extent of overtopping (depth of flow over the crest and the duration of the overtopping flow) which is required for breaching to occur is not an inherent feature of the dam-breach flood models. Some attempts were made to develop erosion models for earthen dams (5,10) however, these were not very adequate. A recent effort by Ponce and Tsivoglou (18) may hold some promise although the difficulties of nonhomogeneity and lack of detailed data for most earthen dams may limit the applicability of this approach. Almost all of the dam-breach models do not address the question of when failure from overtopping commences although a few (8,9,11) utilize a specified depth of overtopping flow to start the formation of the breach.

Breach Characteristics. - A significant source of error is the size, shape, and time of formation of the breach. The few models (8,9,11) which attempt to include the dynamic characteristics of the breach require the user to specify the terminal width, shape and a time of formation which is assumed linear. This information must be obtained from historical dam failures and then applied to the dam being modeled using sound engineering judgement by considering the type of dam (earthfill, rockfill, concrete gravity or arch), the dam's material properties, the cause of failure, the height of the dam, the reservoir volume, and any other special characteristics which might affect the breach formation. An erosion model (18) may in certain instances increase the accuracy of the breach prediction.

Of the three breach characteristics, the shape is least important. Time of formation becomes increasingly insignificant as the reservoir volume becomes very large. The peak discharge (Q_p) emanating from a time-dependent breach can be approximated (28) as:

$$Q_p \simeq 3.1\ W\ [C/(\tau + C/\sqrt{H})]^3 \qquad (1)$$

where: $C = 23.4\ S_a/W$ (2)

in which W is the average breach width (ft), τ is the time (hrs) of breach formation (the time in which the flow passage is enlarging), H is the height (ft) of the dam, and S_a is the reservoir surface area (acres) at the dam crest. Using Eq (1) the peak discharge can be determined for various values of τ, and the sensitivity of Q_p to errors in the time of failure can be determined readily. For example

if, τ=1.5 hr, W=150 ft, S_a=1936 acres, H=262 ft which approximates the Teton dam failure, values of Q_p as a function, of τ are given in Table 1.

Table 1. - Peak Discharge (Q_p) Variations with Time of Failure (τ)

Q_p(cfs)	τ (hr)	Error(%)
1,977,589	0.0	+ 26.1
1,756,766	0.75	+ 12.1
1,567,817	1.5	0.0
1,263,868	3.0	- 19.3

If S_a were 193,600 acres, the error for τ=0. would only be +.2%; whereas, if S_a were only 193.6 acres, a τ=0. would produce a much larger error in Q_p of +487.5%.

Eq (1) can also be used in a similar manner to acertain the effect of error in the average breach width (W). This is a most important source of error. It is most difficult to determine for concrete gravity dams, while its probable value for concrete arch dams is near the full width of the dam. For earthfill dams there is evidence (9,12) that W is somewhat correlated to the dam height (H), i.e.,

$$0.5\ H \leq W \leq 3\ H \qquad (3)$$

At this time the best analysis that can be achieved with such uncertainties in the breach properties is to make two predictions, first using a maximum probable W and minimum probable τ and then using a minimum probable W and maximum probable τ. The first produces a maximum expected downstream flooding while the second produces a minimum expected flooding. This is illustrated in Fig. 1 in which the peak discharge profile is shown for four different conditions. The two lower profiles are associated with the approximated actual downstream valley (Teton-Snake River) dimensions while the two upper profiles are for a narrow canyon (approx. 1100 ft wide) extending throughout the 60 mile downstream reach.

Four properties of dam-breach floods are illustrated by the profiles shown in Fig 1. First, in each case significant differences in the predicted peak flow in the vicinity of the dam are significantly reduced as the flood propagates downstream. Second, the differences are more rapidly reduced for the actual valley (which is very wide and flat having a maximum inundated width of about nine miles) than for the narrow canyon. Third, the peak discharge is rapidly attenuated as the flood advances downstream, and fourth, the peak flow is attenuated more in the wide valley than in the narrow canyon. These general properties are applicable to dam-failure floods; however, the degree of trend of the first three becomes less

as the reservoir volume increases. This is due to the fact that attenuation of the peak discharge becomes less as the volume of the flood wave increases in relation to a fixed storage volume of the downstream valley.

The first principle, the dampening of initial differences in the peak discharge as the flood propagates downstream, enables prediction accuracy to increase in the downstream direction.

The errors in the routed discharge may be transformed into errors in flow depth (h), which are more meaningful, by either using actual depth-discharge rating curves or in the following way. Let the average cross section of the downstream channel-valley be described as:

$$B = kh^m \tag{4}$$

$$A = \frac{kh^{m+1}}{m+1} \tag{5}$$

in which B is the width, A is the cross-sectional area, and k and m are fitting coefficients (see Fig. 1). Then from the Manning Equation,

$$h = (Q/a)^b \tag{6}$$

where: $$a = 1.49\ S^{1/2}\ k/[n(m+1)^{5/3}] \tag{7}$$

$$b = 3/(3m + 5) \tag{8}$$

in which S is the channel-valley slope and n is the Manning roughness coefficient. Using Eq (6), the following ratio may be developed:

$$h_e/h = (Q_e/Q)^b \tag{9}$$

in which the subscript (e) designates quantities possessing some error. Since the fitting coefficient m is present in Eq (9), the general shape of the cross section as determined by m as shown in Fig 1. must be considered. An expression for the percent error in depth (E_h) may be developed in terms of the ratio h_e/h, i.e.,

$$E_h = 100\ (h_e/h - 1) \tag{10}$$

and a similar expression for the percent error in discharge (E_Q), i.e.,

$$E_Q = 100\ (Q_e/Q - 1) \tag{11}$$

Furthermore, the error term (E_h) may be plotted as shown in Fig. 2 against the percent error in the discharge (E_Q) for a range of cross-sectional shapes. Fig. 2 shows that the relationship between E_h and

E_Q is nonlinear. For example, if E_Q = +50% and m=2.0, E_h is determined from Fig. 2 to be about 9.5%. The tendency for an error in flow to yield a smaller error in depth is characteristic of all curves in Fig. 2; this is helpful in promoting prediction accuracy of dam-breach flood routing models. Fig. 2 is based on steady flow, therefore it is strictly applicable only for discharge errors existing after flood routing computations have been performed.

Cross-Sectional Area. - Errors to some extent are always present in the description of the cross-sectional properties (width and area as a function of flow depth) of the downstream channel-valley. These are: errors in sampling, errors in field measurements, and errors inherent in the assumed linear variation between contour intervals of topographic maps. The first two errors are associated with the use of field measured cross-sections while all three errors can occur when using topographic maps for determing cross-sections for a dam-breach flood routing model.

The cross-sectional volume error due to the sampling interval can be eleminated if planmetered surface areas between two selected cross-sections are used to compute the properties of an average section placed between the selected sections. The width ($\overline{B}$) of the average section can be determined from a distance-weighting relationship, e.g.,

$$\overline{B} = (2\ S_c - B_1\Delta x_1 - B_2\Delta x_2)/(\Delta x_1 + \Delta x_2) \tag{12}$$

in which S_c is the surface area contained between contour lines of the same elevation and located on opposite sides of the valley and bounded on the ends by the selected sections designated by subscripts 1 and 2. Also, Δx_1 and Δx_2 are the respective distances (ft) from the first end section to the location of the average section, and from the average section to the second end section. Field measured properties of the cross section within the banks of the channel are needed to reduce errors in this portion of the cross-section since topographic maps do not extend below the typical water level. However, in many cases peak dam-breach flows would have small errors since the in-bank area is a small percentage of the flooded over-bank area.

The error associated with the assumed linear variation between contour intervals (Δh) is illustrated in Fig. 3. An approximate expression for the ratio of A_e/A is given by the following:

$$A_e/A = 1.0 + 0.5\ \overline{P}\ I(m+1)\ (\Delta h/h_p)^{m+1} \tag{13}$$

where: $$\overline{P} = \frac{1}{2N}\sum_{i=1}^{N} e_i = \frac{1}{2N}\sum_{i=1}^{N} \Delta A_i/A_i' \tag{14}$$

$$I = \sum_{i=1}^{N} [i^m - (i-1)^m] \tag{15}$$

$$N \simeq h_p/\Delta h \tag{16}$$

in which Δh is the contour interval, h_p is the maximum depth in the section from Eqs (1) and (6), ΔA_i and A'_i are defined in Fig. 3, and m is defined in Eq (4). A realistic maximum value for the ratio (A_e/A) can be obtained from Eq (13) by using $\bar{P} = 0.4$. From Eq (13) it is seen that larger values of A_e/A and therefore larger errors in the cross-sectional area are directly proportional to m and to the term $(\Delta h/h_p)^{m+1}$. The latter term represents the ratio of contour interval to peak depth. Therefore as the contour interval increases, the error increases. Also, the error increases as the ratio $(\Delta h/h_p)$ increases and since h_p is related to the dam height (H) through Eqs (1) and (16), the error increases as the ratio $\Delta h/H$ increases. The error is related to the cross-sectional shape by the exponent m in the term $(\Delta h/h_p)^{m+1}$.

Using Eq (6), the following ratio may be developed:

$$h_e/h = (A_e/A)^{5b/3} \tag{17}$$

and an expression for percent error in the cross-sectional area (E_A) is given by:

$$E_A = 100\ (A_e/A - 1) \tag{18}$$

The error term E_A may be plotted as shown in Fig 4. against the percent error (E_A) for a range of channel shapes. The relationship is linear for m=0 and becomes more nonlinear as m increases. As m increases the errors become more damped, i.e., if E_A = +50% and m = 2.0, E_h is only +20%.

Flow Resistance Coefficients. - Errors in the flow resistance coefficients are due to such factors as: (1) dam-breach flows which are relatively large occur in previously unflooded areas; thus previous flows are not very useful in computing the flow resistance coefficients; (2) the inundated area often contains more flow resistance in the form of trees, houses, etc. which are not typical of the resistance encountered by most normal floods; (3) the flood-plain flow short-circuits across a meandering channel (4) causing some additional flow resistance; (4) debris (trees, etc.) uplifted and transported by the flood may become impinged on permanent obstructions causing additional undefined flow resistance; and (5) sediment entrapped behind the dam and released during the failure may slightly reduce the flow resistance when it is deposited on the flood plain (4).

The errors associated with the first two factors may be reduced by using a type of Colebrook-White frictional expression which separately approximates effects of submerged and partially submerged objects on the flow resistance (27). The computed Darcy friction factor (f) can then be changed to the more popular Manning n coefficient by using the relation,

$$n = f^{1/2} h^{1/6} / 10.8 \tag{19}$$

The effect that the total error in the frictional resistance (expressed in terms of the Manning n) has on the flood depth can be obtained by using Eq (6). Thus,

$$h_e/h = (n_e/n)^b \tag{20}$$

An expression for the percent error in the Manning n (E_n) may be developed, i.e.,

$$E_n = 100\ (n_e/n - 1) \tag{21}$$

If E_n is plotted against E_h as shown in Fig. 2 it is apparent that the relationship is nonlinear and that errors in the Manning n (E_n) are dampened when transformed into errors in flow depth (E_h) as was also the case with the errors in flow (E_Q). The extent of dampening is directly proportional to the channel shape or the m coefficient of Eq (9). The error dampening characteristic is beneficial for the prediction accuracy of computed depths.

Errors in the Manning n will also have a significant effect on the kinematic celerity (approximate propagation speed) of the flood wave. Using Eq (20), the following celerity ratio can be developed:

$$c_e/c = (n_e/n)^{2b/3 - 1} \tag{22}$$

Eq (22) indicates that errors in the Manning n will produce damped errors in the wave celerity. For example, if E_n = +50% and m = 1.0 the error in the wave celerity would be only -25%. Also, the influence of the cross-section shape factor(m) is very weak in Eq (22). The error in celerity (E_c) is plotted against the error in the friction (E_n) in Fig. 5.

Debris. - Uprooted trees, demolished houses, cars, fences, and other debris transported by the high velocity flow associated with the dam-breach flood cause unpredictable errors. The debris can increase the frictional resistance coefficients. It may also accumulate at constricted cross sections such as bridge openings where it partially or completely restricts the flow as a temporary dam. This occured during the infamous Johnstown dam-breach flood of 1889. At best, the maximum magnitude of this effect can only be approximated by a dam-breach model (9) which treats the blocked constriction as another downstream dam having an estimated head-

discharge rating which somewhat approximates the gradual flow stoppage and the later possible rapid increase if the debris dam is breached. The errors in dam-breach flow predictions caused by debris dams are not predictable since the occurrance, itself, cannot be predicted.

Volume Losses. - Often in dam-breach floods, where the extremely high flows inundate considerable portions of channel overbank or valley flood plain, a measurable loss of flow volume occurs. This is due to infiltration into the relatively dry overbank material, detention storage losses, and sometimes short-circuiting of flows from the main valley into other drainage basins via canals or overtopping natural ridges separating the drainage basins. Such losses of flow are most difficult to predict; usually they are neglected in the dam-breach models, although the losses can be significant. In the case of the Teton flood where the measured losses amounted to about 25% of the reservoir volume, consideration of the losses (8) decreased the routed peak discharge and depth by 50% and 31%, respectively, at a cross-section which had a shape factor(m) of 0.5 and located 60 miles downstream. The average decrease in peak discharge and depth along the 60 mile reach were about 18% and 7%, respectively.

Sediment Transport. - Sediment entrapped behind a breached dam may be transported along with the breach flow and deposited in the downstream valley. In some cases (4) this can reduce the flow resistance coefficient. Also, degradation of the channel bottom may occur due to the high velocity flow emanating from a breached dam. Degradation increases the cross-sectional area of the channel; however, since the channel area is usually small compared to the flooded overbank area the effect on the total flow would be small.

Complex Flow. - The highly turbulent flow in the reach just downstream of the breached dam may not be adequately described by the equations of one-dimensional flow. Also, dam-breach flow that spreads onto a very wide, flat flood plain is subject to some computational error when treated with one-dimensional routing models. In this case, two-dimensional models (13,29) may provide more accuracy; however, at the present time such models are not sufficiently developed for practical and general application, and are functional primarily as research tools.

CONCLUSIONS

In recent years, significant developments have been made in one-dimensional models to predict the flooding due to breached dams; nevertheless, even the more advanced models are limited in their prediction accuracy. The models, when used to reproduce historical dam-failure floods (3,9,16) in which the breach characteristics (shape, size, time of formation) and/or the breach outflow could be adequately approximated, produced errors of about two feet or more in the profile of the flood crest. When the models are used to predict future dam-breach floods, additional significant errors are introduced through the prediction of the breach characteristics and/or the

breach outflow. Perhaps the greatest error in many applications is determining if indeed a dam will be breached. Other errors in the predicted downstream flooding are due to errors in the downstream cross-sectional volume, estimated flow resistance coefficients, undefined effects of transported debris and sediment, undefined flow volume losses, and complex flows that are not well-suited for one-dimensional flow computations.

The errors associated with the breach characteristics do dampen as the flood propagates downstream, and the degree of dampening depends on the cross-sectional shape and the reservoir volume. Also, the percent error in the computed flow depth is less than the percent error in routed discharge, cross-sectional area, and/or flow resistance. Also, there is a dampening of the error in the wave celerity caused by error in the resistance coefficient. These error properties aid in producing the accuracy that is now achievable with dam-breach flood routing models.

APPENDIX 1. - REFERENCES

1. Balloffet, A., Cole, E. and Balloffet, A.F., "Dam Collapse Wave in a River", Journal of the Hydraulics Division, ASCE, Vol. 100, HY5, pp. 645-665, May 1974.
2. Brevard, J.A., and Theurer, F.D., "Simplified Dam-Break Routing Procedure", Technical Release Number 66, U.S. Dept. of Agriculture, Soil Conservation Service, Engr. Div., 35 pp., 1979.
3. Chen, C. and Armbruster, J.T., "Dam-Break Wave Model: Formulation and Verification", Journal of the Hydraulics Division, ASCE, Vol. 106, HY5, pp. 747-767, May 1980.
4. Chen, Y.H. and Simons, D.B., "An Experimental Study of Hydraulic and Geomorphic Changes in an Alluvial Channel Induced by Failure of a Dam", Water Resources Research, Vol. 15, No. 5, pp. 1183-1188, October 1979.
5. Cristofano, E.A., "Method of Computing Rate for Failure of Earthfill Dams". Bureau of Reclamation, Denver, Colo., April, 1965.
6. Cunge, J.A., "Calcul de Propagation des Ondes de Rupture de Barrage (Computation of Dam-Break Waves)", La Houille Blanche, No. 1, 1970.
7. De Saint-Venant, Barre, "Theory of Unsteady Water Flow, with Application to River Floods and to Propagation of Tides in River Channels", Acad. Science (Paris) Comptes rendus, Vol. 73, pp. 237-240, 1871.
8. Fread, D.L., "The Development and Testing of a Dam-Break Flood Forecasting Model", Proceedings, Dam-Break Flood Modeling Workshop, U.S. Water Resources Council, Washington, D.C., pp. 164-197, 1977.
9. Fread, D.L., "Capabilities of NWS Model to Forecast Flash Floods Caused by Dam Failures", Preprint Volume, Second Conference on Flash Floods, March 18-20, Amer. Meteorological Soc., Boston, Mass., pp. 171-178, 1980.
10. Harris, G.W., and Wagner, D.A., "Outflow from Breached Dams", University of Utah, 1967.

11. Hydrologic Engineering Center (HEC), "Flood Hydrograph Package (HEC-1): Users Manual for Dam Safety Investigation", The Hydrologic Engineering Center, Corps of Engineers, U.S. Army, Davis, Cal., 88 pp., Sept. 1978.
12. Johnson, F.A., and Illes, D.A., "A Classification of Dam Failures", Water Power and Dam Construction, pp. 43-45, Dec., 1976.
13. Katapodes, N., and Strelkoff, T., "Two-Dimensional Shallow Water-Wave Models", Journal of the Engineering Mechanics Division, ASCE, Vol. 105, EM2, pp. 317-334, April 1979.
14. Keefer, T.N., and McQuivey, R.S., "Simplified Routing of Dam Break Waves", Proceedings, IAHR, Vol. 2, San Paulo, Brazil, pp. 325-329, 1975.
15. Keefer, T.N., and Simons, R.K., "Qualitative Comparison of Three Dam-Break Routing Models", Proceedings, Dam-Break Flood Modeling Workshop, U.S. Water Resources Council, Washington, D.C., pp. 292-311, 1977.
16. Land, L.F., "Evaluation of Selected Dam-Break Flood-Wave Models by Using Field Data", U.S. Geological Survey Gulf Coast Hydro Science Center, NSTL Station, Miss., Water-Resources Investigations 80-44, 54 pp., July 1980.
17. Middlebrooks, T.A., "Earth-Dam Practice in the United States", Centennial Transactions, ASCE, Paper No. 2620, pp. 697-722, 1952.
18. Ponce, V.M., and Tsivoglou, A.J., "Modeling Gradual Dam Breaches", Journal of the Hydraulics Division, ASCE, Vol. 107, HY6, Paper No. 16371, June 1981.
19. Price, J.T. and Garrison, J.M., "Floodwaves from Hydrologic and Seismic Dam Failures", Paper presented at ASCE National Water Resources Meeting, January 1973.
20. Price, J.T., Lowe, G.W., and Garrison, J.M. "Unsteady Flow Modeling of Dam-Break Waves", Proceedings, Dam-Break Flood Modeling Workshop, U.S. Water Resources Council, Washington, D.C., pp. 90-130.
21. Rajar, R., "Mathematical Simulation of Dam-Break Flow", Journal of the Hydraulics Division, ASCE, Vol. 104, HY7, pp. 1011-1026, July 1978.
22. Ritter, A., "The Propagation of Water Waves", Ver. Deutsch Ingenieure Zeitschr. (Berlin), Vol. 36, Pt. 2, No. 33, pp. 947-954, 1892.
23. Sakkas, J.G., and Strelkoff, T. "Dam Break Flood in a Prismatic Dry Channel", Journal of the Hydraulics Division, ASCE, Vol. 99, HY12, pp. 2195-2216, Dec., 1973.
24. Schoklitsch, A., "On Waves Created by Dam Breaches", Akad. Wiss. (Vienna) Proc., 126, Pt. 2A, pp. 1489-1514, 1917.
25. Snyder, F.F., "Floods from Breaching of Dams". Proceedings, Dam-Break Flood Modelling Workshop, U.S. Water Resources Council, Washington, D.C., pp. 75-85, 1977.
26. Thomas, W.A., "Calculating and Routing of the Teton Dam-Break Flood", Proceedings, Dam-Break Flood Modeling Workshop, U.S. Water Resources Council, Washington, D.C., pp. 198-227, 1977.
27. Walton, R. and Christensen, B.A., "Friction Factors in Storm Surges Over Inland Areas", Journal of Waterway, Port, Coastal and Ocean Division, ASCE, Vol. 106, WW2, pp. 261-271, May 1980.

28. Wetmore, J.N., and Fread, D.L., "The NWS Simplified Dam-Break Flood Forecasting Model", Proceedings, 5th Canadian Hydrotechnical Conference, Fredericton, Canada, 24 pp., May 1981.
29. Xanthopoulous, T., and Koutitas, C., "Numerical Simulation of a Two-Dimensional Flood Wave Propagation Due to Dam Failure", Journal of Hydraulic Research, IAHR, Vol. 14, No. 4, pp. 321-331, 1976.

APPENDIX 2. - NOTATION

The following symbols are used in this paper:

A = cross-sectional area
A_e = cross-sectional area with error
A_i = cross-sectional area defined in Fig. 3
a = coefficient defined by Eq (7)
B = cross-sectional top width
$\overline{B}$ = cross-sectional top width for average section between two end sections
b = coefficient defined by Eq (8)
C = coefficient defined by Eq (2)
c = kinematic wave celerity
c_e = kinematic wave celerity with error
E_A = percent error in cross-sectional area
E_h = percent error in flow depth
E_n = percent error in Manning n
E_Q = percent error in flow
e_i = error in cross-section
f = Darcy friction factor
H = dam height
h = depth of flow
h_e = depth with error
h_p = depth associated with peak flow at a section
k = fitting coefficient for cross-section (scale factor)
m = fitting coefficient for cross-section (shape factor)
N = integer defined by Eq (15)
n = Manning n
n_e = Manning n with error
$\overline{P}$ = cumulative error ratio for cross-section area
Q = flow
Q_e = flow with error
Q_p = peak flow emanating from breached dam
S = channel-valley slope
S_a = surface area of reservoir at height of dam
S_c = surface area of downstream valley reach between two end sections
W = average width of breach
ΔA_i = cross-sectional area (error)
Δh = contour interval
Δx = distance between end section and average section
τ = time for breach formation

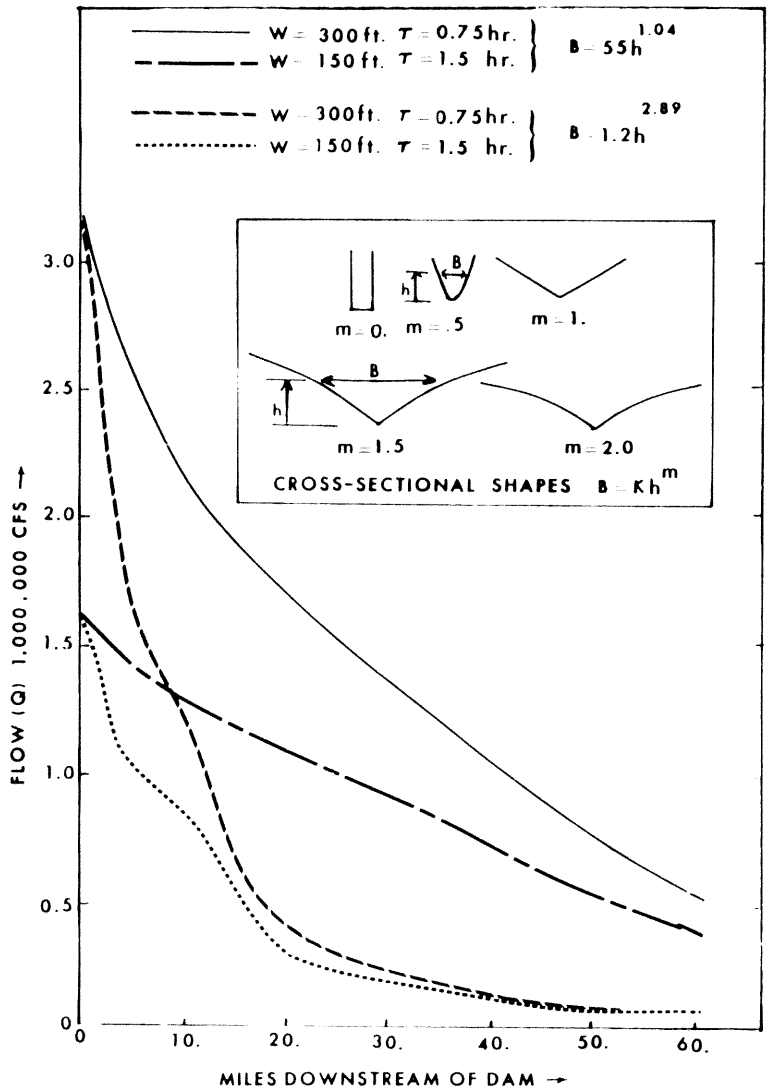

FIG. 1 - VARIATION OF PEAK FLOW DOWNSTREAM OF DAM

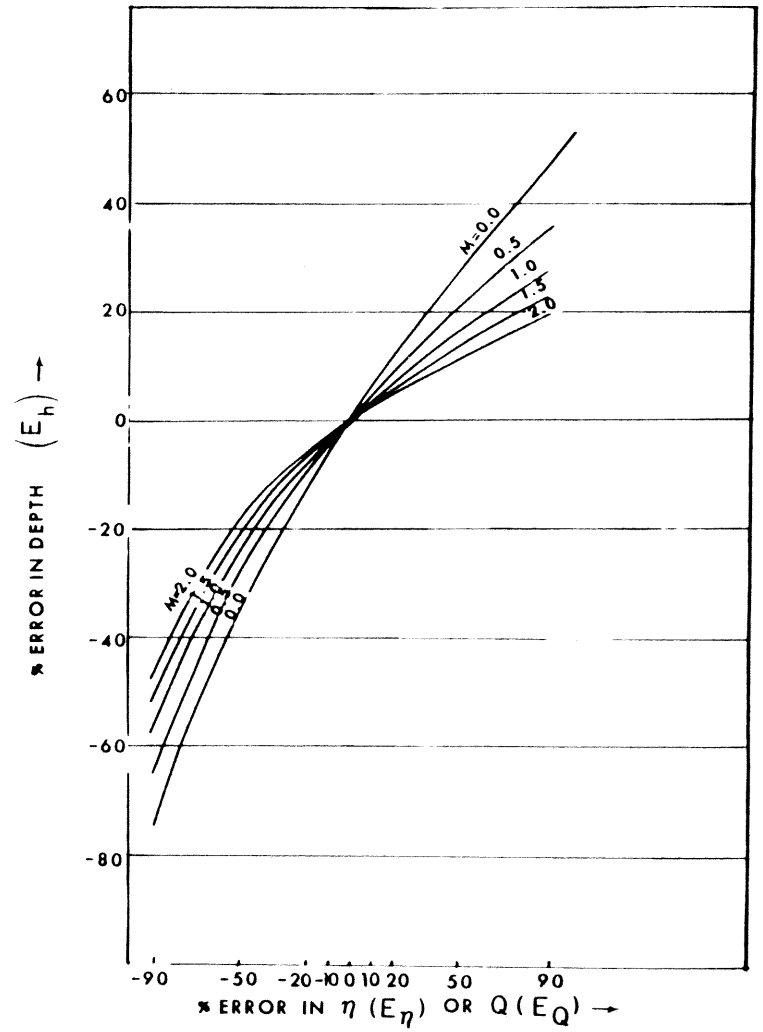

FIG. 2 - ERROR IN FLOOD DEPTH CAUSED BY ERROR IN ROUGHNESS (η) OR FLOW (Q) FOR VARIOUS SHAPED SECTIONS HAVING STEADY FLOW

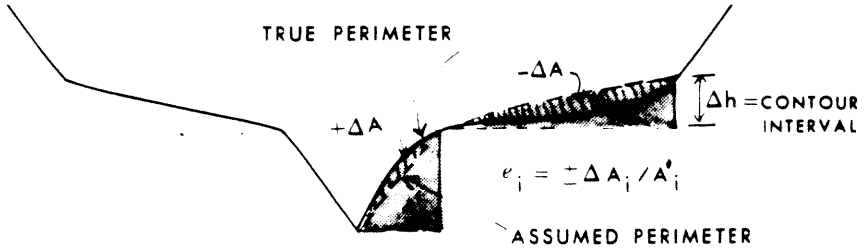

FIG.3-CROSS SECTION SHOWING ERROR $\left(e_i = \pm \Delta A / A'_i\right)$ DUE TO ASSUMED STRAIGHT-LINE VARIATION BETWEEN CONTOUR INTERVALS

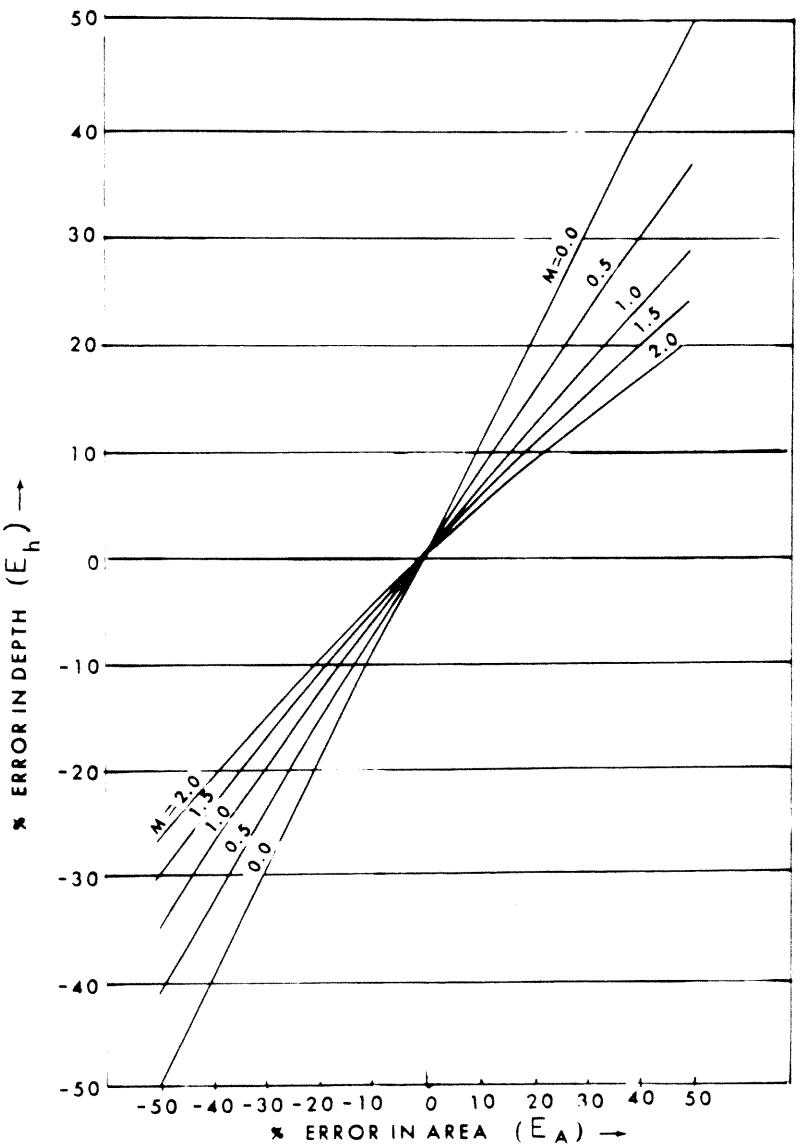

FIG.4-ERROR IN FLOOD DEPTH CAUSED BY ERROR IN CROSS-SECTIONAL AREA FOR VARIOUS SHAPED SECTIONS HAVING STEADY FLOW

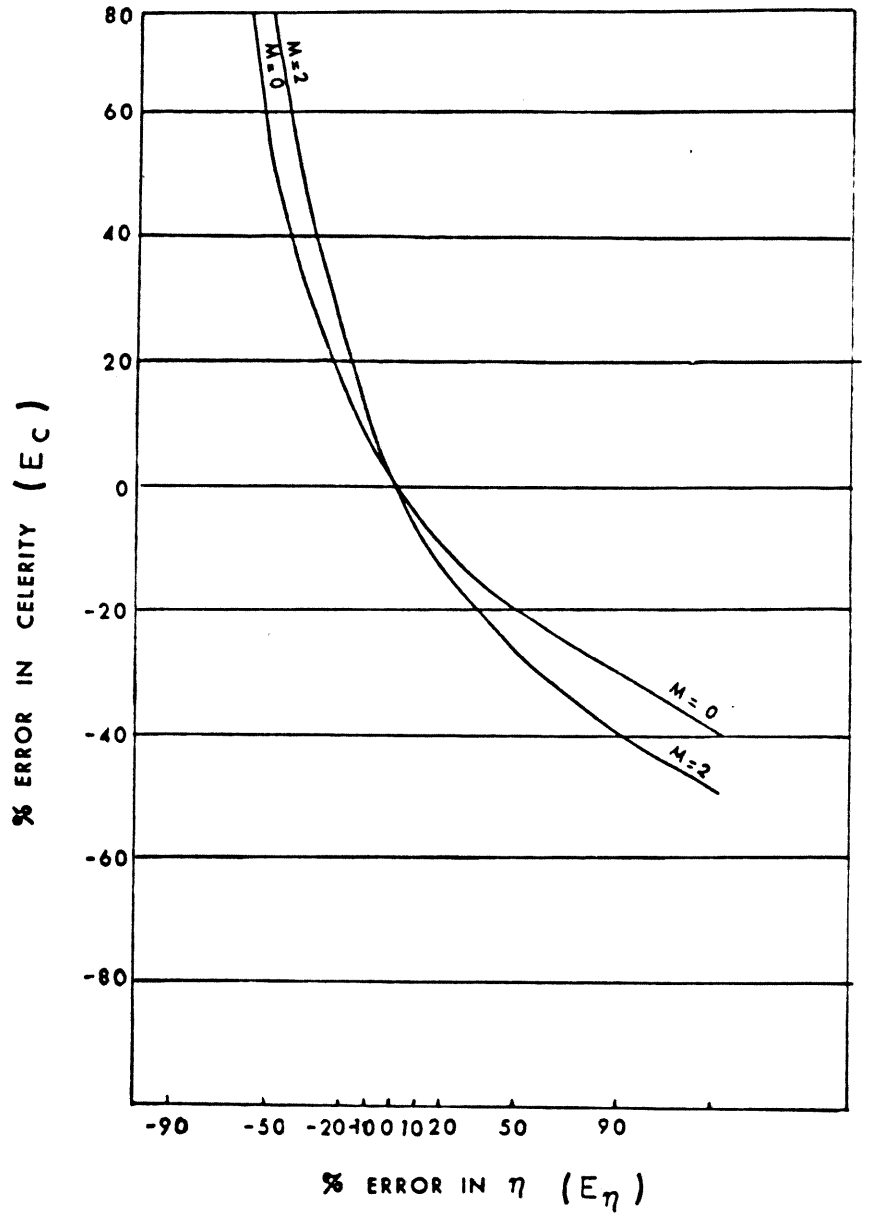

FIG. 5- ERROR IN FLOOD CELERITY CAUSED BY ERROR IN ROUGHNESS FOR VARIOUS SHAPED SECTIONS